

Chromium-Catalyzed CO₂–Epoxide Copolymerization

Joanna Gurnham,[†] Sandro Gambarotta,^{*,†} Ilia Korobkov,[†] Lidia Jasinska-Walc,^{‡,§} and Robbert Duchateau^{*,‡}

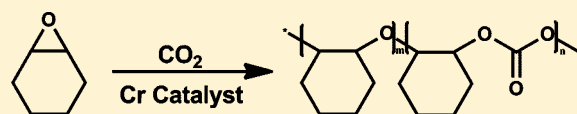
[†]Department of Chemistry, University of Ottawa, Ottawa, Ontario K1N 6N5, Canada

[‡]Department of Chemistry, Eindhoven University of Technology, P.O. Box 513, 5600 MB Eindhoven, The Netherlands

[§]Department of Polymer Technology, Chemical Faculty, Gdansk University of Technology, G. Narutowicza Str. 11/12, 80-233 Gdansk, Poland

S Supporting Information

ABSTRACT: Iminopyrrole, aminopyrrole, and aminophosphine ligands were complexed with various chromium sources, producing eight complexes that were tested for their catalytic behavior toward epoxide–CO₂ copolymerization. As elucidated by MALDI-TOF-MS, copolymerizations afforded polycarbonates and poly(ether-carbonates) exhibiting linear or cyclic topologies.



INTRODUCTION

The possibility of producing biodegradable polycarbonates by copolymerizing CO₂ and epoxide provides an attractive alternative to the technology based on the usage of toxic chemicals such as phosgene.^{1–8} In the search for new catalytic systems, cyclohexene oxide is a convenient comonomer, since it is inexpensive and produces a linear polycarbonate with high tensile strength and a relatively high T_g value of 116 °C.⁹

Although many promising results have stemmed from the study of zinc catalysts for CO₂–epoxide copolymerization,^{8–25} several other metals have been investigated. Among them, trivalent and octahedral chromium²⁶ and cobalt complexes²⁷ have generated remarkable catalytic systems. Although not isolobal, these species share a similar ligand field in the sense that paramagnetic chromium complexes possess a half-filled configuration of the cobalt analogues. In spite of the promising versatility of these catalysts, tetradentate salen,^{16,26,28–45} porphyrin,^{27,46} and related^{47–51} systems, successfully investigated by Darensbourg and Holmes, appear to be the only existing chromium-based catalysts. Naturally, it would be interesting to probe chromium complexes stabilized by different ancillary ligands.

In this broad-scope exploratory study, we have used ligands with the nitrogen donor motif embedded in different functions such as neutral pyridines with aminophosphine pendants, pyrroles with either imine or amine pendants and a combination of them. The reason behind these choices was to use robust ligand systems with little possibility of being leached out or being involved in the reactivity of target molecules. Also, the possibility of tuning steric features was regarded as a bonus in case of we needed to reduce back-biting during the copolymerization cycle.

We herein describe the catalytic behavior of chromium and chromium–zinc complexes of a Ph₂PN(Me)CH₂Py (PyNP) ligand, 1–3, as well as the synthesis of three pyrrole-containing ligands with different donor functions: PyrCHN(ⁿBu)

(Pyr=N), PyrCH₂NH(ⁿBu) (PyrN), and PyCH₂N(ⁿBu)-CH₂Pyr (PyNPyr). All of the corresponding complexes 1–8 have been tested for copolymerization of CO₂ and cyclohexene oxide to poly(cyclohexenecarbonates).

EXPERIMENTAL SECTION

All manipulations were carried out under an inert nitrogen atmosphere using Schlenk glassware or in a drybox. Solvents were dried using an activated alumina purification system. Chemicals were obtained from commercial sources and used as received. DMAP was purchased from Strem and used as received. PPN⁺Cl[−] was purchased from Sigma and used as received. Elemental analyses were carried out by using a PerkinElmer 2400 CHN analyzer. ESI-MS spectrometry was carried out using a MicroMass Q-ToF 1 instrument. Magnetic susceptibilities were measured using a Johnson Matthey magnetic susceptibility balance at room temperature; sample preparation was performed inside a drybox using calibrated, sealed tubes. X-ray crystal data were determined using a Bruker diffractometer equipped with a Smart CCD area detector and with Bruker Kappa APEXII CCD diffractometer. NMR spectra of ligands were recorded on a Bruker Avance 400 MHz spectrometer. Complexes 1 and 2 were prepared according to a described procedure.⁵²

Preparation of Ph₂PN(Me)CH₂Py (PyNP). A solution of 2-[(methylamino)methyl]pyridine (5.0 g, 40 mmol) in THF (100 mL) was cooled to 0 °C, and Et₃N (6.6 mL, 41 mmol) was added. Chlorodiphenylphosphine (7.6 mL, 41 mmol) was added slowly, and the resulting mixture was stirred at room temperature for 48 h. The resulting suspension was filtered and the solvent removed in vacuo. The title product was obtained as an orange oil and used without need for further purification (10.1 g, 33 mmol, 81%). ¹H NMR (400 MHz, CDCl₃): δ 8.51–7.07 (m, 14H (Ph and Py H's)), 4.38 (d, *J* = 9.2 Hz, 2H), 2.51 (d, *J* = 6.4 Hz, 3H). ¹³C NMR (400 MHz, CDCl₃): δ 160.1, 149.1, 139.0, 136.5, 132.2, 128.6, 128.2, 122.0, 121.9, 62.4, 37.4. ³¹P NMR (300 MHz, CDCl₃): δ 67.54 (s).

Preparation of *N*-Butyl-*N*-(1*H*-pyrrolemethylidene)amine (Pyr=N).⁵³ A solution of 1*H*-pyrrole-2-carboxaldehyde (9.5 g, 100

Received: May 26, 2014

Published: August 20, 2014

mmol) in THF (100 mL) was cooled to 0 °C, and butylamine (10.9 mL, 110 mmol) was added dropwise. The solution was stirred at 0 °C for 15 min and then warmed to room temperature and stirred for an additional 12 h. Evaporation of the solvent in vacuo afforded the product as a dark red oil (14.9 g, 100 mmol, 100%). ¹H NMR (400 MHz, CDCl₃): δ 11.37 (s, 1H, N–H), 8.16 (s, 1H), 6.91 (s, 1H), 6.57 (d, *J* = 2.4 Hz, 1H), 6.29 (t, *J* = 3.0 Hz, 1H), 3.64 (t, *J* = 6.8, 2H), 1.68 (m, 2H), 1.44 (m, 2H), 0.98 (t, *J* = 7.4, 3H). ¹³C NMR (400 MHz, CDCl₃): δ 152.1, 130.3, 122.0, 114.2, 109.4, 60.5, 33.3, 20.3, 13.4.

Preparation of 1*H*-Pyrrol-2-ylmethylbutylamine (Pyr-N).⁵³ A solution of *N*-butyl-*N*-(1*H*-pyrrolemethylidene)amine (8.0 g, 53 mmol) in distilled methanol (80 mL) was cooled to 0 °C, and excess NaBH₄ (4.0 g, 105 mmol) was added slowly. Gas evolution was observed. The resulting brown suspension was stirred at room temperature overnight and then concentrated to 50 mL in vacuo. The excess NaBH₄ was quenched with 50 mL of water, and the aqueous solution was extracted three times with diethyl ether (3 × 30 mL). The combined Et₂O fractions were dried over MgSO₄ and filtered, and the solvent was evaporated in vacuo, affording the product as a red-orange oil (6.89 g, 45 mmol, 70%). ¹H NMR (400 MHz, CDCl₃): δ 10.04 (s, 1H N–H pyrrole), 6.76 (s, 1H), 6.21 (s, 1H), 6.15 (s, 1H), 3.86 (s, 2H), 2.74 (t, *J* = 7.2 Hz, 2H), 1.60 (m, 2H), 1.46 (m, 2H), 1.03 (t, *J* = 7.2, 3H). ¹³C NMR (400 MHz, CDCl₃): δ 130.4, 117.5, 107.8, 106.4, 49.2, 46.7, 32.0, 20.5, 14.0.

Preparation of *N*-Butyl-*N*-(2-pyridylmethyl)-*N*-(1*H*-2-pyrrolylmethyl)amine (Py-N-Pyr).⁵³ A suspension of Na₂CO₃ (7.7 g, 4.0 mmol) in water (12 mL) was added to 100 mL of cooled (0 °C) methanol. To the resulting suspension, was added picolyl chloride hydrochloride (3.8 g, 23 mmol), and the mixture was stirred at 0 °C for 2 h while a pink suspension was formed. Neat 1*H*-pyrrol-2-ylmethylbutylamine (3.5 g, 23 mmol) was added to the pink suspension, and stirring was continued at room temperature for 5 days. The color slowly changed from pink to pale orange. The suspension was filtered and the filtrate collected and concentrated in vacuo. The resulting solution was washed with chloroform (3 × 15 mL), and the chloroform fractions were combined and dried over MgSO₄. After filtration and solvent evaporation in vacuo, a yellow oil was obtained and purified by column chromatography over silica-60H with 10% MeOH/90% CHCl₃ (1.73 g, 7.13 mmol, 31%). ¹H NMR (400 MHz, CDCl₃): δ 9.82 (broad s, NH), 8.55 (d, *J* = 4 Hz, 1H), 7.66 (m, 1H), 7.42 (d, *J* = 8, 1H), 7.18 (m, 1H), 6.78 (m, 1H), 6.13 (m, 1H), 6.03 (s, 1H), 3.89 (s, 2H), 3.58 (s, 2H), 2.48 (t, *J* = 6.4, 2H), 1.53 (m, 2H), 1.30 (m, 2H), 0.88 (t, *J* = 7.2, 3H). ¹³C NMR (400 MHz, CDCl₃): δ 159.4, 148.8, 136.7, 128.1, 124.1, 122.2, 117.3, 107.7, 107.6, 58.9, 54.0, 49.3, 29.4, 20.6, 14.1.

Preparation of (PyrN)Zn(CH₂CH₃)Cr(CH₂CH₃)Cl₂ (3). A solution of **1** (0.27 g, 0.50 mmol) in toluene (5 mL) was cooled to –30 °C for about 5 min, and then Zn(CH₂CH₃)₂ was added dropwise (0.31 g, 2.5 mmol) and the resultant dark green solution was stirred at room temperature for 20 min. The insoluble solid material was discarded by centrifugation, and the resulting solution was cooled to –30 °C for 4 days. Blue block-shaped crystals of **3** were isolated and washed with cold hexanes (3 × 2 mL) and dried (0.19 g, 0.26 mmol, 52%). $\mu_{\text{eff}} = 3.88 \mu_{\text{B}}$. Anal. Calcd (found) for C₂₂H₃₈Cl₄Cr₂N₄Zn₂: C, 35.94 (36.69); H, 5.21 (4.22); N, 7.62 (7.06).

Preparation of (Pyr=N)₂CrCl(THF) (4). A solution of Pyr=N (0.15 g, 1 mmol) in THF (5.0 mL) was treated with KH (0.04 g, 1.1 mmol) and the mixture stirred at room temperature for 12 h. The resulting pale red suspension was treated with CrCl₃(THF)₃ (0.19 g, 0.5 mmol) and stirred at room temperature for 12 h. The color changed to dark red. The crude material was dried in vacuo, redissolved in hexane (5.0 mL), and separated from KCl via centrifugation. The product was recrystallized from hexane at –35 °C, yielding small red crystals of **4** suitable for X-ray analysis (0.18 g, 0.4 mmol, 53%). $\mu_{\text{eff}} = 3.78 \mu_{\text{B}}$. Anal. Calcd (found) for C₂₇H₃₇CrN₆: C, 64.91 (64.08); H, 7.87 (7.33); N, 16.82 (15.93).

Preparation of (PyrN)CrCl₂(THF)₂ (5). A solution of PyrN (0.15 g, 1 mmol) in THF (5.0 mL) was treated with KH (0.09 g, 2.2 mmol), and the mixture was stirred at room temperature for 12 h. The resulting peach-colored suspension was treated with Cr(acac)₃ (0.35 g,

1.0 mmol) and stirred at room temperature for 12 h. The color changed to dark red-brown. The crude material obtained upon drying the reaction mixture in vacuo was redissolved in toluene (5.0 mL) and separated from KCl via centrifugation. The product was recrystallized from toluene at –35 °C, yielding red crystals of **5** (0.31 g, 0.67 mmol, 67%). $\mu_{\text{eff}} = 3.63 \mu_{\text{B}}$. ESI-MS calcd (found): 420.1380 (420.2056). Anal. Calcd (found) for C₁₇H₃₁Cl₂CrN₂O₂: C, 49.04 (49.86); H, 7.02 (7.17); N, 6.73 (7.29).

Preparation of (PyrN)Cr(acac)₂ (6). A solution of PyrN (0.23 g, 1.5 mmol) in THF (7.0 mL) was treated with KH (0.13 g, 3.3 mmol), and the mixture was stirred at room temperature for 12 h. The resulting golden yellow suspension was treated with Cr(acac)₃ (0.52 g, 1.5 mmol) and stirred at room temperature for 12 h. The color changed to dark red-brown, and the mixture was evaporated to dryness. The crude material was further dried in vacuo, redissolved in toluene (5.0 mL), and separated from K(acac) via centrifugation. The product was recrystallized from toluene at –35 °C, yielding red crystals of **6** suitable for X-ray diffraction (0.21 g, 0.5 mmol, 35%). $\mu_{\text{eff}} = 3.62 \mu_{\text{B}}$. Anal. Calcd (found) for C₁₉H₂₈CrN₂O₄: C, 56.85 (55.95); H, 7.28 (7.09); N, 6.98 (7.35).

Preparation of (PyrNPY)CrCl₂(THF) (7). A solution of PyrNPY (0.97 g, 4.0 mmol) in THF (20.0 mL) was treated with KH (0.18 g, 4.4 mmol), and the mixture was stirred at room temperature for 12 h. The resulting dark red-brown solution was treated with CrCl₃(THF)₃ (1.5 g, 4.0 mmol) and stirred at room temperature for 12 h, while the color changed to dark green. The material was dried in vacuo and the residue redissolved in toluene (12.0 mL) and separated from KCl via centrifugation. The product was recrystallized from toluene at –35 °C, yielding small green crystals of **7** (0.87 g, 2.0 mmol, 50%). $\mu_{\text{eff}} = 3.83 \mu_{\text{B}}$. ESI-MS calcd (found): 367.1716 (367.2263). Anal. Calcd (found) for C₂₁H₃₁Cl₃CrN₂OP: C, 52.30 (52.97); H, 6.24 (6.15); N, 9.63 (9.02).

Preparation of (PyrNPY)Cr(acac)₂ (8). A solution of PyrNPY (0.24 g, 1 mmol) in THF 8.0 mL was treated with KH (0.04 g, 1.1 mmol), and the mixture was stirred at room temperature for 12 h. The resulting dark red-brown solution was treated with Cr(acac)₃ (0.35 g, 1.0 mmol) and stirred at room temperature for 12 h, while the color changed to dark brown. The crude material was dried in vacuo, redissolved in toluene (6.0 mL), and separated from K(acac) via centrifugation. The product was recrystallized from toluene at –35 °C, yielding small brown crystals of **8** (0.31 g, 0.63 mmol, 63%). $\mu_{\text{eff}} = 3.73 \mu_{\text{B}}$. ESI-MS calcd (found): 491.1877 (491.3080). Anal. Calcd (found) for C₂₁H₃₁Cl₃CrN₂OP (found): C, 60.96 (60.50); H, 6.96 (6.76); N, 8.53 (7.91).

Polymerization Methods. The copolymerizations were performed both in bulk and in solution with a [cyclohexene oxide:catalyst:cocatalyst] ratio of [500:1:1], unless stated otherwise.

Bulk. A mixture of cyclohexene oxide (5.09 mmol) and catalyst (10.19 μmol) and cocatalyst (10.19 μmol) was reacted in a 5 mL glass sleeve equipped with a stirring bar and placed inside a bomb reactor and pressurized with 50 bar of CO₂. The reactor was placed in an oil bath on a stirrer/heating plate. The polymerization was conducted at 80 °C, unless stated otherwise. All analyses were performed on crude samples.

Solution. A 5 mL glass sleeve equipped with a stirring bar was placed inside a bomb reactor and charged with a mixture of CHO (5.095 mmol), catalyst (10.19 μmol), and cocatalyst (10.19 μmol) in toluene (1 mL) and pressurized with 50 bar of CO₂. The reactor was placed in an oil bath and mounted on top of a stirrer/heating plate. Polymerization was conducted at 80 °C, unless stated otherwise. All analyses were performed on crude samples.

Analysis of Polymers. NMR spectra were recorded on a Varian Mercury Vx (400 MHz) spectrometer at 25 °C in chloroform-*d*, and ¹H NMR spectra were referenced internally using residual solvent proton signals. For ¹H NMR experiments, the spectral width was 6402.0 Hz, the acquisition time was 1.998 s, and the number of recorded scans was equal to 64. SEC analyses were carried out using a Waters 2695 separations module, a Model 2414 refractive index detector (at 40 °C), and a Model 486 UV detector (at 254 nm) in series. Injections were done by a Waters Model WISP 712

autoinjector, using an injection volume of 50 mL. The columns used were a PLgel guard (5 μm particles) 50 \times 705 mm column, followed by two PLgel mixed-C (5 μm particles) 300 \times 7.5 mm columns at 40 $^\circ\text{C}$ in series. Tetrahydrofuran (THF stabilized with BHT, Biosolve) with 1% v/v acetic acid was used as eluent at a flow rate of 1.0 mL min^{-1} . The molecular weights were calculated with respect to polystyrene standards (Polymer Laboratories, $M_p = 580$ Da up to $M_p = 7.1 \times 10^6$ Da). Before SEC analysis was performed, the samples were filtered through a 0.2 μm PTFE filter (13 mm, PP housing, Alltech). MALDI-TOF-MS analyses were performed on a Voyager DE-STR instrument from Applied Biosystems equipped with a 337 nm nitrogen laser. An accelerating voltage of 25 kV was applied. Mass spectra of 1000 shots were accumulated. The polymer samples were dissolved in CHCl_3 at a concentration of 1 mg mL^{-1} . The cationization agent used was potassium trifluoroacetate (Fluka >99%) dissolved in THF at a concentration of 5 mg mL^{-1} . The matrix used was *trans*-2-[3-(4-*tert*-butylphenyl)-2-methyl-2-propenyldiene]malononitrile (DCTB) (Fluka) and was dissolved in THF at a concentration of 40 mg mL^{-1} . Solutions of matrix salt and polymer were mixed in a volume ratio of 4:1:4. The mixed solution was hand spotted on a stainless steel MALDI-TOF-MS target plate and left to dry. The spectra were recorded in the reflection mode. All MALDI-TOF-MS spectra were recorded from the crude products. Software developed in house was used to characterize the polymers in detail and allow elucidation of the individual chain structures, the copolymer's chemical composition, and topology.

X-ray Crystallography. Data collection results for compounds **3**, **4**, **6**, and **9** represent the best data sets obtained in several trials for each sample. The crystals were mounted on thin glass fibers using paraffin oil. Crystals were cooled to 200 K prior to data collection. Data were obtained with a Bruker AXS KAPPA single-crystal diffractometer equipped with a sealed Mo tube source (wavelength 0.71073 \AA) APEX II CCD detector. Raw data collection and processing were performed with the APEX II software package from BRUKER AXS.⁵⁴ Diffraction data for **3**, **4**, and **9** were collected with a sequence of 0.5 $^\circ$ ω scans at 0, 120, and 240 $^\circ$ in ϕ . Due to lower unit cell symmetry and in order to ensure adequate data redundancy, diffraction data for **6** were collected with a sequence of 0.5 $^\circ$ ω scans at 0, 90, 180, and 270 $^\circ$ in ϕ . Initial unit cell parameters were determined from 60 data frames with 0.3 $^\circ$ ω scan each, collected at different sections of the Ewald sphere. Semiempirical absorption corrections based on equivalent reflections were applied.⁵⁵ Systematic absences in the diffraction data set and unit cell parameters were consistent with orthorhombic *Pbca* (No. 61) for **4**, triclinic $P\bar{1}$ (No. 2) for **6**, and monoclinic $P2_1/n$ (alternative setting for No. 14, $P2_1/c$) for **3** and **9**. Solutions in the centrosymmetric space groups for all three compounds yielded chemically reasonable and computationally stable refinement results. The structures were solved by direct methods, completed with difference Fourier synthesis, and refined with full-matrix least-squares procedures based on F^2 .

All four structural models contain molecules of the target compounds situated in the general positions.

The structural model of **3** displays one molecule of the target compound located on the inversion center symmetry element of the space group. The compound structure appears to be a dimer with asymmetric unit containing only half of the molecule. All the atoms in the structural model were refined with full set of anisotropic displacement parameters.

Diffraction data for the crystal of **4** were collected to 0.75 \AA resolution. However, due to small crystal size and weak diffraction it was discovered that both $R(\text{int})$ and $R(\sigma)$ exceed 35% for the data below 1.10 \AA resolution. On the basis of the $R(\sigma)$ value data were truncated to 1.00 \AA resolution for structure solution and refinement. On the final refinement stages for the structural model of **4** it was noticed that, when the atoms were refined with a full set of anisotropic displacement parameters, the thermal motion parameters for two *n*-Bu fragments based at C(15) and C(24) suggested the presence of positional disorder not related to symmetry elements of the crystal space group. Positional disorder was introduced for positions from C(16) to C(18) and from C(24) to C(27) of the *n*-butyl substituents.

Initially occupational factors for all disordered atoms were allowed to refine. However, on the final stages of structure refinement occupational factors were restrained to 50:50 values for both disordered fragment. Several sets of geometry restraints (DFIX, DANG) were introduced to ensure acceptable molecular geometry for these moieties. To obtain acceptable values of thermal motion parameters and avoid further splitting of atomic positions, sets of thermal parameters constrains (SIMU, RIGU) were introduced into the refinement routine. Introduction of thermal motion restraints allowed successful anisotropic refinement for all disordered atomic positions.

Diffraction data for the crystal of complex **6** were collected to 0.75 \AA resolution. However, due to small crystal size and weak diffraction it was discovered that both $R(\text{int})$ and $R(\sigma)$ exceed 35% for the data below 0.95 \AA resolution. On the basis of the $R(\sigma)$ value data were truncated to 0.90 \AA resolution for structure solution and refinement.

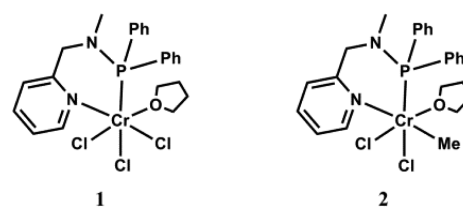
For all of the compounds, all hydrogen atom positions were calculated on the basis of the geometry of the related non-hydrogen atoms. All hydrogen atoms were treated as idealized contributions during the refinement. All scattering factors are contained in several versions of the SHELXTL 2013 program library.⁵⁶

RESULTS AND DISCUSSION

As discussed above, polycarbonate synthesis requires Lewis acidic catalysts with a nucleophilic initiator group to aid in a coordination–insertion mechanism of epoxide and CO_2 .^{1–3,7} The chromium–alkyl function might provide a good nucleophilic initiator that can dissociate from the metal center to facilitate the epoxide's ring opening. Chromium complexes have previously been used as Lewis acidic polycarbonate catalysts,^{26,27} however, the most popular metal used for such reactions remains zinc.^{2,14–20,22,23,66–70} Therefore, the possibility of combining chromium with organoaluminum or possibly -zinc in a multimetallic cluster was interesting because of the possibility of following a bimetallic mechanism^{71,72} while maintaining a metal–alkyl initiating function.

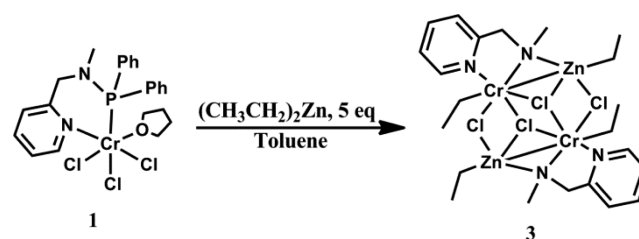
The synthesis and characterization of the $\text{PyCH}_2\text{N}(\text{CH}_3)\text{-PPH}_2$ ligand and complexes **1** and **2** have been previously reported (Scheme 1).⁵²

Scheme 1



To prepare heterobimetallic catalytic systems, we have reacted **1** with a variety of aluminum alkyl reagents, systematically obtaining ill-defined materials. We have thus explored the reaction with diethylzinc (Scheme 2). The

Scheme 2



paramagnetism of the complex made uncertain any structural characterization via NMR. Since blue block-shaped crystals were obtained in this case, the connectivity was determined by an X-ray crystal structure (Figure 1). The complex is

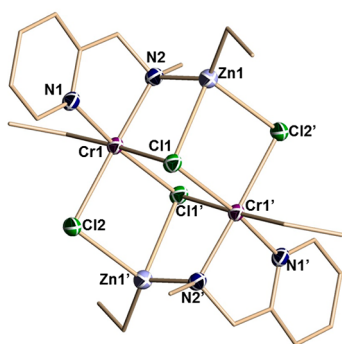


Figure 1. Drawing of **3** with thermal ellipsoids drawn at 50% probability. Select bond lengths (Å) and angles (deg) of **3**: Cr1–Cl1 2.3931(3), Cr1–Cl1' 2.7097(3), Cr1–Cl2 2.4122(3), Cr1–C8 2.068(1), Cr1–N1 2.0535(9), Zn1–Cl1 2.5389(3), Zn1–N2 2.032(1); Cl1'–Cr1–Cl1 87.62(1), Cl2–Cr–Cl1 85.53(1), C8–Cr–Cl1 94.43(4), N1–Cr–N2 81.24(4), Cl2'–Zn–Cl1 85.14(1), N2–Zn1–Cl1 92.62(3).

tetrametallic with two trivalent organochromium centers and two zinc moieties connected by bridging chlorides. The structure may be described as an edge-sharing bioctahedral dichromium with two bridging chlorines. The two tetrahedral zinc atoms fill the two pockets generated by two chlorines and the ligand's amino nitrogen atom. The Ph₂P unit of the ligand has been eliminated during the reaction, most likely as a result of the nucleophilic attack of one diethylzinc unit.

Having lost this phosphine residue, the ligand became monoanionic. Although this is surprising, this transformation has been observed before.^{57,58} The chromium center has retained the trivalent state and, even more surprisingly, formed a seemingly stable bond with an ethyl group. This group is coplanar with the Cr₂Cl₂ core.

The preparation of the other ligands used in this work started with the synthesis of Pyr(CH)N(CH₂)₃CH₃ (Pyr=N) via condensation of 1*H*-pyrrole-2-carboxaldehyde with butylamine. Subsequent reduction with NaBH₄ afforded Pyr(CH₂)NH(CH₂)₃CH₃ (Pyr-N). In turn, treatment of the Pyr-N ligand with Na₂CO₃ and picolyl hydrochloride afforded Py(CH₂)N-(butyl)(CH₂)Pyr (Py-N-Pyr).

The ligand Pyr=N was complexed with chromium trichloride (Scheme 3) to form a red crystalline material (**4**). The X-ray crystal structure determination revealed coordination of this species in a ligand:chromium ratio of 3:1 (Figure 2).

Each ligand is monoanionic and contains two donor nitrogen atoms, resulting in a typical octahedral geometry of Cr(III).

Scheme 3

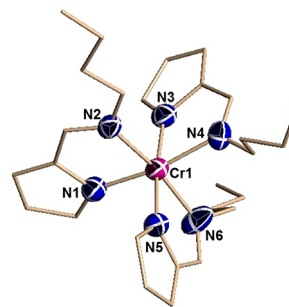
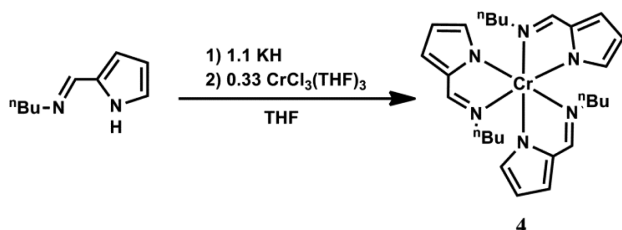
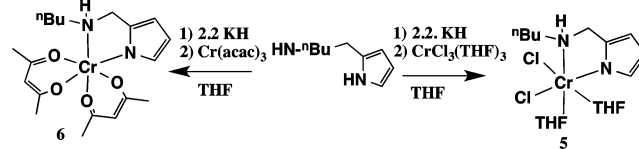


Figure 2. Partial thermal ellipsoid drawing for **4** at 50% probability. Select bond lengths (Å) and angles (deg) of **4**: Cr1–N3 2.006(5), Cr1–N5 2.028(5), Cr1–N6 2.055(5), Cr1–N2 2.069(5), Cr1–N4 2.070(5); N3–Cr1–N1 89.8(2), N3–Cr1–N5 174.6(2), N1–Cr1–N5 93.9(2), N3–Cr1–N6 96.0(2), N5–Cr1–N6 79.8(2).

Also, when the reaction was carried out with ligand:chromium ratios of 1:1 and 2:1, complex **4** was the only characterized product. All bond lengths and angles of this chlorine-free complex are within the expected range.

When Pyr-N was complexed with chromium trichloride, a brown, microcrystalline material unsuitable for X-ray analysis was obtained (Scheme 4). Characterization was therefore

Scheme 4



carried out with ESI-MS, IR, and magnetic susceptibility measurements, indicating the presence of a single deprotonated ligand on a chromium metal center, with two chlorine atoms (thus maintaining the +3 oxidation state) and two molecules of THF to complete the coordination sphere (**5**).

The reaction of the potassium salt of Pyr-N with Cr(acac)₃ as a different chromium source in THF afforded a red-brown crystalline material (Scheme 4). The crystal structure determination showed ligand coordination via the two nitrogen donors, the chromium coordination sphere being completed by two molecules of acetylacetonate (Figure 3).

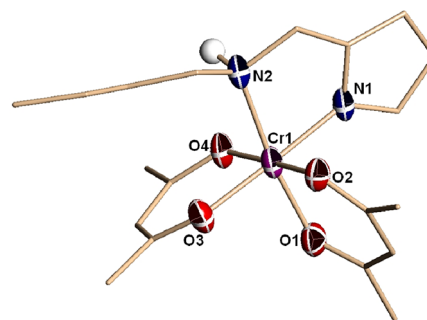
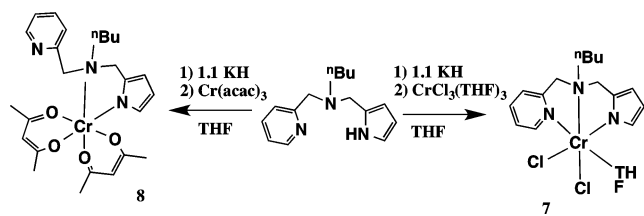


Figure 3. Partial thermal ellipsoid drawing for **6** at 50% probability. Select bond lengths (Å) and angles (deg) of **6**: Cr1–O1 1.952(3), Cr1–O2 1.958(3), Cr1–N1 1.991(3), Cr1–N2 2.120(4); O1–Cr1–O2 91.91(13), O2–Cr1–O4 176.57(12), O1–Cr1–N1 92.18(14), O3–Cr1–N1 175.7(15), O3–Cr1–N2 96.55(13), N1–Cr1–N2 80.04(15).

The pyramidal geometry of the nitrogen atom indicates that no deprotonation occurred. Accordingly, the IR spectrum showed a band at 3176 cm^{-1} expected for the N–H stretching vibration, confirming the presence of the N–H group. Furthermore, the magnetic susceptibility measurement confirms the presence of chromium in the +3 oxidation state. All bond lengths and bond angles were within the expected range.

The reaction of the potassium salt of Py-N-Pyr with $\text{CrCl}_3(\text{THF})_3$ in THF afforded a green microcrystalline material. Unfortunately, numerous attempts to grow suitable crystals for X-ray diffraction were unsuccessful. Therefore, we propose the structure 7 on the grounds of analytical and magnetic data (Scheme 5). Furthermore, the Py-N-Pyr ligand

Scheme 5

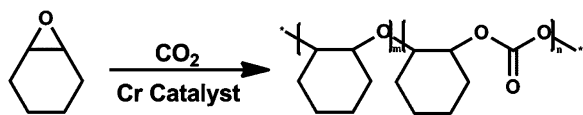


has a “bite” somehow reminiscent of Sasol’s $\text{HN}(\text{CH}_2\text{CH}_2\text{PR}_2)_2$ ⁵⁹ and $\text{HN}(\text{CH}_2\text{CH}_2\text{SR})_2$,⁶⁰ also tridentate ligands with two-carbon bridges between the donor atoms. Due to these similarities, we suggest that coordination will occur in the same way providing analogous facial configuration, with a five-membered chelating ligand surrounding an octahedral, trivalent chromium.^{59–61}

The reaction of the potassium salt of Py-N-Pyr with a different chromium source, $\text{Cr}(\text{acac})_3$, in THF afforded a brown microcrystalline material, which we proposed to have the structure 8. Analytical data were in agreement with the proposed formulation (Scheme 5).

Some of the complexes (4, 6, 8) do not seem to have the right structural motifs to be active catalysts for the epoxide– CO_2 copolymerization, since they lack a rather labile nucleophilic substituent such as a chloride. Thus, all of the complexes were tested in combination with 4-dimethylamino-pyridine (DMAP) or bis(triphenylphosphine)iminium chloride (PPN^+Cl^-) as cocatalyst. Upon testing the analytically pure isolated complexes for their catalytic behavior in cyclohexene oxide CHO– CO_2 copolymerization (Scheme 6), we found

Scheme 6



complexes 1 and 2 showed some polymerization activity, producing a low-molecular-weight polycarbonate with moderate TOFs. Complex 2 contains a chromium–alkyl function, and upon testing in toluene using bis(triphenylphosphine)iminium chloride as a cocatalyst, up to 76% conversion of CHO to polycarbonate was obtained (Table 1, entry 10). When the reaction using bis(triphenylphosphine)iminium chloride as a cocatalyst was performed in the absence of solvent, there was still 60% conversion of CHO to polycarbonate (entry 7).

Regardless of the cocatalyst used, complex 1 showed the highest degree of polymerization activity of the pyridine-NP based catalysts, with up to 90% conversion of CHO to a low molecular-weight polycarbonate (Table 1, entries 1 and 3). In the absence of cocatalysts, complex 1 still showed 76% conversion of CHO to low-molecular-weight polycarbonate (entry 5). Complexes 1 and 2 both produced similar low-molecular-weight polymers with low PDIs. Both complexes displayed the same selectivity toward polycarbonate production, but complex 2 exhibited lower activity, likely due to the instability of the chromium–alkyl bond, which could have decomposed in situ or via reaction with the cocatalyst.

When the reaction time was shortened from 18 h to only 4 h, no conversion of CHO was observed, even when the concentration of CHO was increased (entries 8 and 9), indicating an induction time of at least 4 h.

Disappointingly, complex 3 showed no conversion of CHO to polycarbonate at all under various conditions (Table 1, entries 12–16). When tested in THF (entry 17), a 22% conversion of CHO was observed due to higher solubility; however, only 11% carbonate linkages were produced, indicating that this catalyst mainly homopolymerizes cyclohexene oxide to the corresponding polyether.

Upon testing the chlorine-free catalyst 4 for polymerization activity, polycarbonates in a molecular weight range (up to 3670) higher than that of 1–3 were formed (Table 2). After 4 h, a low-molecular-weight polymer was produced with 50% carbonate linkages and a rather low conversion of CHO (Table 2, entry 1). This is not surprising, since 4 does not have the right structural motif to be a catalytically active species and, most probably, residual water present in the system hydrolyzes off one of the supporting ligands. That water is present in our system, most probably carried by CO_2 , is also clear from the low-molecular-weight products that we generally obtained. Water initiation, leading to low-molecular-weight products, is a well-known phenomenon in epoxide– CO_2 copolymerization. When the reaction time was increased to 8 h, TOF, molecular weight, and percent carbonate linkages all increased. The CHO conversion to polycarbonate increases with increasing reaction time. Interestingly, after 32 h the reaction progress reached a plateau at 74% CHO conversion, most likely caused by catalyst deactivation (Figure 4). Figure 5 shows that the average concentration of carbonate linkages in the polymer also increases over the time of the reaction, again reaching a plateau after 32 h (Figure 5). When the polymerization temperature was lowered from 80 to 60 °C (Table 2, entry 6), a decrease in TOF was observed, while at 100 °C (entry 5) both TOF and molecular weight increased in comparison to the polymerization at 80 °C. Unfortunately, at this elevated temperature, there was significant production of cyclic cyclohexene polycarbonate. Other changes in the reaction conditions were tested, including different CHO:catalyst:cocatalyst ratios and different cocatalysts, but no significant changes were observed (entries 7 and 8).

Complexes 5 and 6 were prepared from the same aminopyrrole ligand with different chromium precursors with the purpose of obtaining chlorinated and chlorine-free catalysts. Complex 5 produced low-molecular-weight polycarbonates (Table 3, entries 1–8). When the temperature was increased to 100 °C, the molecular weight increased to 3800 (entry 6); however, the PDI increased as well. In all cases, the polymers synthesized by catalyst 5 contained over 50% carbonate linkages.

Table 1. CO₂-Epoxide Copolymerization Results of PyNP Complexes^a

entry	cat.	cocat.	reacn time (h)	solvent	conversn CHO (%) ^b	M _n ^c	PDI ^c	CO ₃ (%) ^b	TOF (h ⁻¹) ^b
1	1	DMAP	18	PhMe	90	1910	1.4	94	25
2	1	PPN ⁺ Cl ⁻	18		63	1450	1.4	91	18
3	1	PPN ⁺ Cl ⁻	18	PhMe	90	1250	1.3	94	25
4 ^d	1	PPN ⁺ Cl ⁻	18	PhMe	81	1630	1.4	93	23
5	1		18	PhMe	76	934	1.3	82	21
6	2	DMAP	18		14	1220	1.3	90	4
7	2	PPN ⁺ Cl ⁻	18		60	1380	1.3	90	17
8	2	PPN ⁺ Cl ⁻	4	PhMe					
9 ^d	2	PPN ⁺ Cl ⁻	4	PhMe					
10	2	PPN ⁺ Cl ⁻	18	PhMe	76	1350	1.3	82	21
11 ^d	2	PPN ⁺ Cl ⁻	18	PhMe	31	1600	1.3	65	17
12	3	DMAP	18						
13	3	PPN ⁺ Cl ⁻	18						
14	3	PPN ⁺ Cl ⁻	4						
15	3	PPN ⁺ Cl ⁻	18	PhMe	1				
16 ^d	3	PPN ⁺ Cl ⁻	18	PhMe					
17	3	PPN ⁺ Cl ⁻	4	THF	22	24240	3.7	11	28

^aConditions: loading 10 μmol of complex, 80 °C, 50 bar of CO₂. DMAP = 4-dimethylaminopyridine, PPN⁺Cl⁻ = bis(triphenylphosphine) iminium chloride. [CHO:cat.:cocat.] = 500:1:1. ^bCarbonate content, calculated from ¹H NMR spectra. ^cSEC performed in THF against PS standards. ^d[CHO:cat.:cocat.] = 1000:1:1.

Table 2. CO₂-Epoxide Copolymerization Results for Complex 4^a

entry	cat.	cocat.	reacn time (h)	solvent	conversn CHO (%) ^b	M _n ^c	PDI ^c	CO ₃ (%) ^b	TOF (h ⁻¹) ^b
1	4	PPN ⁺ Cl ⁻	4	PhMe	33	820	1.1	53	42
2	4	PPN ⁺ Cl ⁻	4		52	3360	1.50	89	65
3	4	PPN ⁺ Cl ⁻	8	PhMe	45	1470	1.50	66	29
4	4	PPN ⁺ Cl ⁻	8		65	2670	1.3	87	40
5 ^d	4	PPN ⁺ Cl ⁻	8		75	3670	1.9	91	47
6 ^e	4	PPN ⁺ Cl ⁻	8		52	1300	1.4	84	33
7	4	DMAP	8		60	2100	1.2	90	38
8 ^f	4	PPN ⁺ Cl ⁻	4		14	1390	1.5	85	34
9	4	PPN ⁺ Cl ⁻	16	PhMe	65	1960	1.2	69	21
10	4	PPN ⁺ Cl ⁻	32	PhMe	74	2240	1.2	74	12
11	4	PPN ⁺ Cl ⁻	72	PhMe	74	2480	1.2	74	12

^aConditions: loading 10 μmol of complex, 80 °C, 50 bar of CO₂. DMAP = 4-dimethylaminopyridine, PPN⁺Cl⁻ = bis(triphenylphosphine) iminium chloride. [CHO:cat.:cocat.] = 500:1:1. ^bCarbonate content, calculated from ¹H NMR spectra. ^cSEC performed in THF against PS standards. ^dT = 100 °C. ^eT = 60 °C. ^f[CHO:cat.:cocat.] = 1000:1:1.

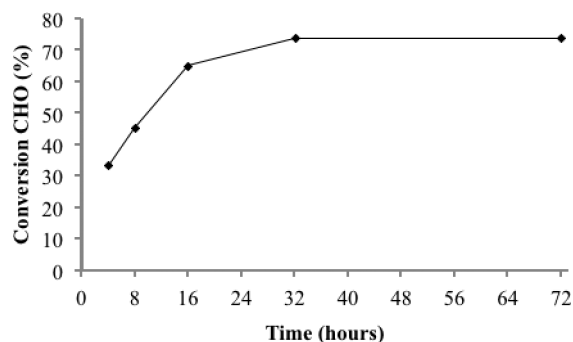


Figure 4. Graphical representation of conversion of cyclohexene oxide (%) as a function of time, catalyzed by complex 4. Reactions were run in toluene at 80 °C and 50 bar of CO₂ with PPN⁺Cl⁻ as a cocatalyst. [CHO:cat.:cocat.] = [500:1:1].

Catalyst 6, similar to catalyst 4, contains no chlorine, and it is unlikely that an acac or pyrrole-amine ligand will be a suitable nucleophilic initiating group. Upon testing, we obtained higher molecular weight polymers than the chlorinated analogue, as well as higher TOFs. When the polymerization reaction

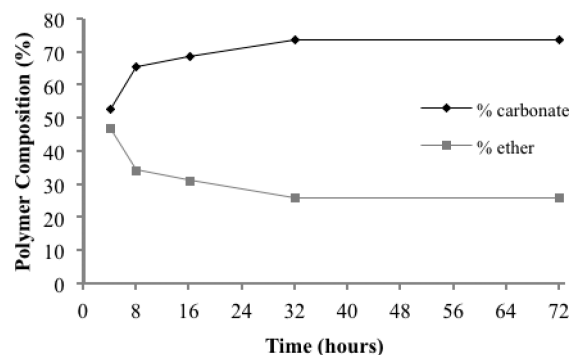


Figure 5. Graphical representation of percent carbonate linkages versus percent ether linkages as a function of time, catalyzed by complex 4. Reactions were run in toluene at 80 °C and 50 bar of CO₂ with PPN⁺Cl⁻ as a cocatalyst. [CHO:cat.:cocat.] = [500:1:1].

proceeded for 8 h (Table 3, entry 11), high conversion of CHO to polymer was observed, producing polymer with an M_n value of 6000 with 83% carbonate linkages. The reaction time was extended, and after 32 h complete conversion of CHO to

Table 3. CO₂-Epoxide Copolymerization Results for Complexes 5 and 6^a

entry	cat.	cocat.	reacn time (h)	solvent	conversn CHO (%) ^b	M _n ^c	PDI ^c	CO ₃ (%) ^b	TOF (h ⁻¹) ^b
1	5	PPN ⁺ Cl ⁻	4	PhMe	18	1460	1.3	54	30
2	5	PPN ⁺ Cl ⁻	4		17	1040	1.1	55	29
3	5	PPN ⁺ Cl ⁻	8	PhMe	18	1530	1.3	72	17
4	5	PPN ⁺ Cl ⁻	8		65	1620	1.6	70	46
5	5	DMAP	8						
6 ^d	5	PPN ⁺ Cl ⁻	8		75	3800	3.3	92	48
7 ^e	5	PPN ⁺ Cl ⁻	8		2	1080	1.3	94	2
8 ^f	5	PPN ⁺ Cl ⁻	4		4	1040	1.2	61	5
9	6	PPN ⁺ Cl ⁻	4	PhMe	43	2700	1.7	77	55
10	6	PPN ⁺ Cl ⁻	4		71	2440	1.4	88	88
11	6	PPN ⁺ Cl ⁻	8	PhMe	79	6010	1.7	83	51
12	6	PPN ⁺ Cl ⁻	8		81	4070	1.7	90	52
13 ^d	6	PPN ⁺ Cl ⁻	8		84	4040	1.8	90	53
14 ^e	6	PPN ⁺ Cl ⁻	8		6	1030	1.3	66	6
15	6	DMAP	8	PhMe	2	700	1.1	52	2
16 ^f	6	PPN ⁺ Cl ⁻	8	PhMe	49	8630	1.6	96	63
17	6	PPN ⁺ Cl ⁻	4	THF	53	3180	1.4	78	67
18	6		4	PhMe					
19	6	PPN ⁺ Cl ⁻	16	PhMe	83	5970	1.4	87	26
20	6	PPN ⁺ Cl ⁻	32	PhMe	99	6550	2.8	93	15

^aConditions: loading 10 μmol of complex, 80 °C, 50 bar of CO₂. DMAP = 4-dimethylaminopyridine, PPN⁺Cl⁻ = bis(triphenylphosphine)iminium chloride. [CHO:cat.:cocat.] = [500:1:1]. ^bCarbonate content, calculated from ¹H NMR spectra. ^cSEC performed in THF against PS standards. ^dT = 100 °C. ^eT = 60 °C. ^f[CHO:cat.:cocat.] = [1000:1:1].

polycarbonate was observed, as depicted in Figure 6. The percentage of carbonate linkages was also found to increase

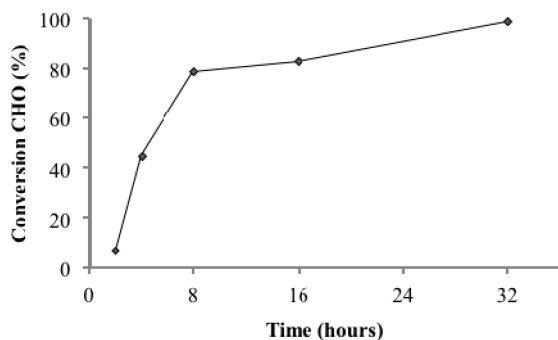


Figure 6. Graphical representation of conversion of cyclohexene oxide (%) as a function of time, catalyzed by complex 6. Reactions run were in toluene at 80 °C and 50 bar of CO₂ with PPN⁺Cl⁻ as a cocatalyst. [CHO:cat.:cocat.] = [500:1:1].

over time, reaching 93% after 32 h (Figure 7). Complexes 7 and 8 are both based on the same pyridine-amino-pyrrole ligand, and, similar to the case for complexes 5 and 6, were complexed with different chromium sources, producing both chlorinated and chlorine-free chromium catalysts. Contrary to our expectations for similar results, much lower activities were observed for 7 and 8 (Table 4). Both catalysts produced only low-molecular-weight products, and in the case of catalyst 8, the products were just oligomers. This is not completely unexpected, taking into account that 8 itself can hardly be expected to be catalytically active and will need to undergo some initiation reaction, probably hydrolysis of one of the ancillary ligands, before polymerization can take place. It is also not unlikely that in this case the cocatalyst in the presence of traces of water provides poor activation. In addition, the conversion of CHO to polymer was low. When the process was

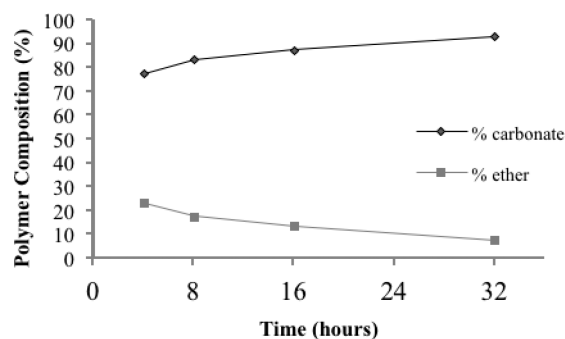


Figure 7. Graphical representation of percent carbonate linkages versus percent ether linkages as a function of time, catalyzed by complex 6. Reactions were run in toluene at 80 °C and 50 bar of CO₂ with PPN⁺Cl⁻ as a cocatalyst. [CHO:cat.:cocat.] = [500:1:1].

tested in THF (entries 5 and 10), the conversion increased due to higher solubility, and the molecular weight increased from the oligomer range to low-molecular-weight polymer. In all cases, the molecular weights of the polymers observed were considerably lower than the calculated MW values for a living system. MALDI-TOF-MS revealed the formation of either cyclic structures or the combination of cyclohexyl/cyclohexenyl end groups as formed by water initiation.⁷⁴

In conclusion, we have surveyed a few chromium complexes of pyrrole and pyridine-based ligand systems for activity as CO₂-epoxide copolymerization catalysts, finding that they may act as catalysts with interesting behavior in some cases. It should be reiterated that, to date, there have been very few examples of chromium catalysts for polycarbonate synthesis in the literature. Among the catalysts presented in this work, complexes 4 and 6 showed the best activity, producing moderate-molecular-weight polymers with a high percentage of carbonate linkages and moderate TOFs. Interestingly, these two catalysts contained no chlorine, and therefore the only

Table 4. CO₂-Epoxide Copolymerization Results for Complexes 7 and 8^a

entry	cat.	cocat.	reacn time (h)	solvent	conversn	CHO (%) ^b	M _n ^c	PDI ^c	CO ₃ (%) ^b	TOF (h ⁻¹) ^b
1	7	PPN ⁺ Cl ⁻	4	PhMe		6	790	1.3	50	19
2	7	PPN ⁺ Cl ⁻	4							
3	7	PPN ⁺ Cl ⁻	8	PhMe		29	1680	1.3	72	24
4	7	PPN ⁺ Cl ⁻	8							
5	7	PPN ⁺ Cl ⁻	4	THF		67	2430	1.2	71	84
6	8	PPN ⁺ Cl ⁻	4	PhMe		2	520	1.0	70	18
7	8	PPN ⁺ Cl ⁻	4			9	650	1.3	55	39
8	8	PPN ⁺ Cl ⁻	8	PhMe		5	580	1.1	55	10
9	8	PPN ⁺ Cl ⁻	8			11	620	1.1	62	12
10	8	PPN ⁺ Cl ⁻	4	THF		52	1750	1.2	81	65

^aConditions: loading 10 μmol of complex, 80 °C, 50 bar of CO₂. DMAP = 4-dimethylaminopyridine, PPN⁺Cl⁻ = bis(triphenylphosphine)iminium chloride. [CHO:cat.:cocat.] = [500:1:1]. ^bCarbonate content, calculated from ¹H NMR spectra. ^cSEC performed in THF against PS standards.

chlorine in the system was introduced by the cocatalyst. Further investigations are in progress to determine the effect of chlorinated versus nonchlorinated catalysts in the copolymerization of CO₂ and epoxides.

■ ASSOCIATED CONTENT

Supporting Information

Tables and CIF files giving crystallographic data for compounds 3, 4, and 6. This material is available free of charge via the Internet at <http://pubs.acs.org>.

■ AUTHOR INFORMATION

Corresponding Authors

*E-mail for S.G.: sgambaro@uottawa.ca.

*E-mail for R.D.: r.duchateau@tue.nl.

Notes

The authors declare no competing financial interest.

■ ACKNOWLEDGMENTS

This work was supported by the NSERC and the Eindhoven University of Technology.

■ REFERENCES

- (1) Kember, M. R.; Buchard, A.; Williams, C. K. *Chem. Commun.* **2011**, *47*, 141–163.
- (2) (a) Darensbourg, D. J. *Chem. Rev.* **2007**, *107*, 2388–410. (b) Childers, M. I.; Longo, J. M.; van Zee, N. J.; LaPointe, A. M.; Coates, G. W. *Chem. Rev.* **2014**, DOI: 10.1021/cr400725x.
- (3) (a) Coates, G. W.; Moore, D. R. *Angew. Chem., Int. Ed.* **2004**, *43*, 6618–6639. (b) Wu, G. P.; Ren, W. M.; Luo, Y.; Li, B.; Zhang, W. Z.; Lu, X. B. *J. Am. Chem. Soc.* **2012**, *134*, 5682–5688. (c) Liu, J.; Ren, W. M.; Liu, Y.; Lu, X. B. *Macromolecules* **2013**, *46*, 1343–1349. (d) Nishioka, K.; Goto, H.; Sugimoto, H. *Macromolecules* **2012**, *45*, 8172–8192.
- (4) Fukuoka, S.; Fukawa, I.; Tojo, M.; Oonishi, K.; Hachiya, H.; Aminaka, M.; Hasegawa, K.; Komiya, K. *Catal. Surv. Asia* **2010**, *14*, 146–163.
- (5) Kember, M. R.; Williams, C. K. *J. Am. Chem. Soc.* **2012**, *134*, 15676–15679.
- (6) Nelson, A. M.; Long, T. E. *Polym. Int.* **2012**, *61*, 1485–1491.
- (7) Klaus, S.; Lehenmeier, M. W.; Anderson, C. E.; Rieger, B. *Coord. Chem. Rev.* **2011**, *255*, 1460–1479.
- (8) (a) Inoue, S.; Tsuruta, T.; Koinuma, H. *J. Polym. Sci., Part B: Polym. Phys.* **1969**, *7*, 287–292. (b) Deglmann, P.; Brym, A. K.; Dengler, J.; Lutz-Kahler, P.; Warzelhan, V.; Rieger, B.; Klaus, S.; Lehenmeier, M. (BASF SE, Germany) WO 2012139994 A1, 2012.
- (9) (a) Koning, C.; Wildeson, J.; Parton, R.; Plum, B.; Steeman, P.; Darensbourg, D. *Polymer* **2001**, *42*, 3995–4004.
- (10) Bolm, C.; Beckmann, O.; Dabard, O. a. G. *Angew. Chem., Int. Ed.* **1999**, *38*, 907–909.
- (11) Takeda, N.; Inoue, S. *Macromol. Chem.* **1978**, *179*, 1377–1381.
- (12) Holtcamp, M. W.; Darensbourg, D. J. *Macromolecules* **1995**, *28*, 7577–7579.
- (13) Darensbourg, D. J.; Holtcamp, M. W.; Struck, G. E.; Zimmer, M. S.; Niezgod, S. a.; Rainey, P.; Robertson, J. B.; Draper, J. D.; Reibenspies, J. H. *J. Am. Chem. Soc.* **1999**, *121*, 107–116.
- (14) Darensbourg, D. J.; Wildeson, J. R.; Yarbrough, J. C.; Reibenspies, J. H. *J. Am. Chem. Soc.* **2000**, 12487–12496.
- (15) Darensbourg, D. J.; Zimmer, M. S.; Rainey, P.; Larkins, D. L. *Inorg. Chem.* **2000**, *39*, 1578–1585.
- (16) Darensbourg, D. J.; Yarbrough, J. C. *J. Am. Chem. Soc.* **2002**, *124*, 6335–6342.
- (17) Dinger, M. B.; Scott, M. J. *Inorg. Chem.* **2001**, *40*, 1029–1036.
- (18) Darensbourg, D. J.; Wildeson, J. R.; Yarbrough, J. C. *Inorg. Chem.* **2002**, *41*, 973–980.
- (19) Darensbourg, D. J.; Rainey, P.; Yarbrough, J. *Inorg. Chem.* **2001**, *40*, 986–993.
- (20) Cheng, M.; Moore, D. R.; Reczek, J. J.; Chamberlain, B. M.; Lobkovsky, E. B.; Coates, G. W. *J. Am. Chem. Soc.* **2001**, *123*, 8738–8749.
- (21) Cheng, M.; Lobkovsky, E. B.; Coates, G. W. *J. Am. Chem. Soc.* **1998**, *120*, 11018–11019.
- (22) Allen, S. D.; Moore, D. R.; Lobkovsky, E. B.; Coates, G. W. *J. Am. Chem. Soc.* **2002**, *124*, 14284–14285.
- (23) Moore, D. R.; Cheng, M.; Lobkovsky, E. B.; Coates, G. W. *J. Am. Chem. Soc.* **2003**, *125*, 11911–11924.
- (24) York, N.; Bastide, J.; Hamelin, J.; Moore, D. R.; Cheng, M.; Lobkovsky, E. B.; Coates, G. W. *Angew. Chem., Int. Ed.* **2002**, *41*, 2599–2602.
- (25) Sakata, K.; Ueno, A.; Jibuta, T.; Hashimoto, M. *Synth. React. Inorg. Met.-Org. Chem.* **1993**, *23*, 1107–1115.
- (26) Darensbourg, D. J.; Mackiewicz, R. M. *J. Am. Chem. Soc.* **2005**, *127*, 14026–14038.
- (27) (a) Mang, S.; Cooper, A. I.; Colclough, M. E.; Chauhan, N.; Holmes, A. B. *Macromolecules* **2000**, *33*, 303–308. (b) Wu, G. P.; Ren, W. M.; Luo, Y.; Li, B.; Zhang, W. Z.; Lu, X. B. *J. Am. Chem. Soc.* **2012**, *134*, 5682–5688. (c) Liu, J.; Ren, W. M.; Liu, Y.; Lu, X. B. *Macromolecules* **2013**, *46*, 1343–1349.
- (28) Darensbourg, D. J.; Yarbrough, J. C.; Ortiz, C.; Fang, C. *J. Am. Chem. Soc.* **2003**, *125*, 7586–7591.
- (29) Darensbourg, D. J.; Mackiewicz, R. M.; Rodgers, J. L.; Phelps, A. L. *Inorg. Chem.* **2004**, *43*, 1831–1833.
- (30) Darensbourg, D. J.; Rodgers, J. L.; Mackiewicz, R. M.; Phelps, A. L. *Catal. Today* **2004**, *98*, 485–492.
- (31) Darensbourg, D. J.; Bottarelli, P.; Andreatta, J. *Macromolecules* **2007**, *40*, 7727–7729.
- (32) Hongfa, C.; Tian, J.; Andreatta, J.; Darensbourg, D. J.; Bergbreiter, D. *Chem. Commun.* **2008**, 975–977.
- (33) Darensbourg, D. J.; Moncada, A. *Inorg. Chem.* **2008**, *47*, 10000–10008.

- (34) Darensbourg, D. J.; Ulusoy, M.; Karroonnirum, O.; Poland, R.; Reibenspies, J. H.; Cetinkaya, B. *Macromolecules* **2009**, *42*, 6992–6998.
- (35) Alvaro, M.; Baleizao, C.; Das, D.; Carbonell, E.; Garcia, H. *Catalysis* **2004**, *228*, 254–258.
- (36) Luinstra, G.; Haas, G.; Molnar, F.; Bernhart, V.; Eberhardt, R.; Rieger, B. *Chem. Eur. J.* **2005**, *11*, 6298–6314.
- (37) Xu, X.; Wang, C.-M.; Li, H.-R.; Wang, Y.; Sun, W.-L.; Shen, Z.-Q. *Polymer* **2007**, *48*, 3921–3924.
- (38) Eberhardt, R.; Rieger, B.; Allmendinger, M. *Macromol. Rapid Commun.* **2003**, *24*, 194–196.
- (39) Darensbourg, D. J.; Mackiewicz, R. M.; Billodeaux, D. R. *Organometallics* **2005**, *24*, 144–148.
- (40) Darensbourg, D. J.; Phelps, A. L. *Inorg. Chem.* **2005**, *44*, 4622–4629.
- (41) Rao, D.-Y.; Li, B.; Zhang, R.; Wang, H.; Lu, X.-B. *Inorg. Chem.* **2009**, *48*, 2830–2836.
- (42) Guo, L.-P.; Wang, C.-M.; Zhao, W.-J.; Li, H.-R.; Sun, W.-L.; Shen, Z.-Q. *Dalton Trans.* **2009**, 5406–5410.
- (43) Li, B.; Zhang, R.; Lu, X.-B. *Macromolecules* **2007**, *40*, 2303–2307.
- (44) Niu, Y.; Zhang, W.; Pang, X.; Chen, X.; Zhuang, X.; Jing, X. *J. Polym. Sci., Part A: Polym. Chem.* **2007**, *45*, 5050–5056.
- (45) Nakano, K.; Nakamura, M.; Nozaki, K. *Macromolecules* **2009**, *42*, 6972–6980.
- (46) Stamp, L. M.; Mang, S.; Holmes, A. B.; Knights, K.; DeMiguel, Y. R.; McConvey, I. F. *Chem. Commun.* **2001**, 2502–2503.
- (47) Darensbourg, D. J.; Fitch, S. *Inorg. Chem.* **2007**, *46*, 5474–5476.
- (48) Darensbourg, D. J.; Fitch, S. *Inorg. Chem.* **2008**, *47*, 11868–11878.
- (49) Darensbourg, D. J.; Fitch, S. *Inorg. Chem.* **2009**, *48*, 8668–8677.
- (50) Vagin, S. I.; Reichardt, R.; Klaus, S.; Rieger, B. *J. Am. Chem. Soc.* **2010**, *132*, 14367–14369.
- (51) Klaus, S.; Vagin, S. I.; Lehenmeier, M. W.; Deglmann, P.; Brym, A. K.; Rieger, B. *Macromolecules* **2011**, *44*, 9508–9516.
- (52) Yang, Y.; Gurham, J.; Liu, B.; Duchateau, R.; Gambarotta, S.; Korobkov, I. *Organometallics* **2014**, DOI: 10.1021/om5003683.
- (53) Bruin, B. de; Kicken, R. J. N. A. M.; Suos, N. F. A.; Gelder, D.; Donners, M. P. J.; Reijer, C. J. den; Sandee, A. J.; Smits, J. M. M.; Gal, A. W.; Spek, A. L. *Eur. J. Inorg. Chem.* **1999**, 1581–1592.
- (54) APEX Software Suite v.2010; Bruker AXS, Madison, WI, 2005.
- (55) Blessing, R. H. *Acta Crystallogr., Sect. A: Found. Crystallogr.* **1995**, *51*, 33–38.
- (56) Sheldrick, G. M. *Acta Crystallogr., Sect. A: Found. Crystallogr.* **2008**, *64*, 112–22.
- (57) Shaikh, Y.; Gurnham, J.; Albahily, K.; Gambarotta, S.; Korobkov, I. *Organometallics* **2012**, *31*, 7427–7433.
- (58) Albahily, K.; Ahmed, Z.; Gambarotta, S.; Koc, E.; Duchateau, R. *Organometallics* **2011**, *30*, 6022–6027.
- (59) McGuinness, D. S.; Wasserscheid, P.; Keim, W.; Hu, C.; Englert, U.; Dixon, J. T.; Grove, C. *Chem. Commun.* **2003**, *49*, 334–335.
- (60) McGuinness, D. S.; Wasserscheid, P.; Keim, W.; Morgan, D.; Dixon, J. T.; Bollmann, A.; Maumela, H.; Hess, F.; Englert, U. *J. Am. Chem. Soc.* **2003**, *125*, 5272–5273.
- (61) McGuinness, D. S.; Wasserscheid, P.; Morgan, D. H.; Dixon, J. T. *Organometallics* **2005**, *24*, 552–556.
- (62) Temple, C.; Jabri, A.; Crewdson, P.; Gambarotta, S.; Korobkov, I.; Duchateau, R. *Angew. Chem., Int. Ed.* **2006**, *45*, 7050–7053.
- (63) Jabri, A.; Temple, C.; Crewdson, P.; Gambarotta, S.; Korobkov, I.; Duchateau, R. *J. Am. Chem. Soc.* **2006**, *128*, 9238–9247.
- (64) Albahily, K.; Koç, E.; Al-Baldawi, D.; Savard, D.; Gambarotta, S.; Burchell, T. J.; Duchateau, R. *Angew. Chem., Int. Ed.* **2008**, *47*, 5816–5819.
- (65) Jabri, A.; Crewdson, P.; Gambarotta, S.; Korobkov, I.; Duchateau, R. *Organometallics* **2006**, *25*, 715–718.
- (66) Darensbourg, D. J.; Lewis, S. J.; Rodgers, J. L.; Yarbrough, J. C. *Inorg. Chem.* **2003**, *42*, 581–589.
- (67) Cheng, M.; Darling, N. a.; Lobkovsky, E. B.; Coates, G. W. *Chem. Commun.* **2000**, 2007–2008.
- (68) Allen, S. D.; Moore, D. R.; Lobkovsky, E. B.; Coates, G. W. *J. Organomet. Chem.* **2003**, *683*, 137–148.
- (69) Darensbourg, D. J.; Wildeson, J. R.; Yarbrough, J. C. *Organometallic* **2001**, *20*, 4413–4417.
- (70) Kember, M. R.; Knight, P. D.; Reung, P. T. R.; Williams, C. K. *Angew. Chem., Int. Ed.* **2009**, *48*, 931–933.
- (71) (a) Cheng, M.; Lobkovsky, E. B.; Coates, G. W. *J. Am. Chem. Soc.* **1998**, *120*, 11018–11019. (b) Cheng, M.; Moore, D. R.; Reczek, J. J.; Chamberlain, B. M.; Lobkovsky, E. B.; Coates, G. W. *J. Am. Chem. Soc.* **2001**, *23*, 8738–8749. (c) Moore, D. R.; Cheng, M.; Lobkovsky, E. B.; Coates, G. W. *J. Am. Chem. Soc.* **2003**, *125*, 11911–11924. (d) Allen, S. D.; Moore, D. R.; Lobkovsky, E. B.; Coates, G. W. *J. Am. Chem. Soc.* **2002**, *124*, 14284–14285.
- (72) Buchard, A.; Jutz, F.; Kember, M. R.; White, A. J. P.; Rzepa, H. S.; Williams, C. K. *Macromolecules* **2012**, *45*, 6781–6795.
- (73) Klaus, S.; Lehenmeier, M. W.; Anderson, C. E.; Rieger, B. *Coord. Chem. Rev.* **2011**, *255*, 1460–1479.
- (74) Duchateau, R.; van Meerendonk, W. J.; Yajjou, L.; Staal, B. B. P.; Koning, C. E.; Gruter, G. J. M. *Macromolecules* **2006**, *39*, 7900–7908.